第 48 卷 第 10 期/2021 年 5 月/中国激光 研究论文

中国激光

电磁辅助激光单道焊接 30 mm 厚板研究

陈根余[1,2*]，王竟如[1]，齐毅[3]，李玮[1]，钟沛新[1]，董理[1]

[1]湖南大学激光研究所，湖南 长沙 410082；

[2]湖南大学汽车车身先进设计制造国家重点实验室，湖南 长沙 410082；

[3]湖北文理学院机械工程学院，湖北 襄阳 441100

摘要 针对激光单道焊接厚板过程中因根部熔池滴落造成焊缝难以成型的问题，提出稳定磁场和电流产生的向上安培力对根部熔池进行辅助支撑焊接厚板的方法。实验结果表明单独电流或磁场的存在对厚板焊接熔池滴落行为影响很小，但引入安培力后根部熔池滴落得到抑制，改善了熔池流动性，焊接过程更加稳定，焊缝成型质量良好，呈现 Y 字型。相同的激光功率等工艺参数条件下，改变安培力大小和方向可以有效控制焊缝的深度，扩展了焊缝质量控制工艺参数。该方法极大地提高了厚板的焊接效率和焊接质量，为解决激光单道焊接厚板“要么不透，一透就漏”的难题提供了新的工艺方法，单道焊接厚度达到 30 mm。

关键词 激光加工；激光焊接；电磁场；厚板；熔池滴落

中图分类号 TG456.7 **文献标志码** A **doi**：10.3788/CJL202148.1002102

1 引 言

激光焊接技术凭借激光能量密度高、焊接效率高和焊接质量好等优点，已经成为机械加工领域极具潜力的焊接技术之一[1-2]。激光单道焊接双面成型技术具有焊缝变形小、焊缝强度高、焊缝深宽比大和焊接效率高的优点[3]，但由于激光功率的限制，一直未能在厚板焊接领域得到应用。经过半个世纪的发展，高质量高功率的激光器不断取得突破，目前光纤激光器最高功率可达 100 kW[4]。一般情况下，单道焊接双面成型良好的板材极限厚度为 13 mm，板材厚度达到 15 mm 以上时，最大的难题已不再是如何优化工艺参数获取良好焊缝，而是激光功率一旦超过阈值，匙孔内激光能量、蒸汽、等离子体等耦合行为复杂，导致根部熔池发生滴落，焊缝难以成型，即存在“要么不透，一透就漏”的世界性难题[5-7]。

2009 年德国联邦材料研究所（BAM）将交变电磁焊接技术成功应用于厚板焊接，发现电磁力对根部的驼峰有抑制作用，并且可以改变焊缝形貌[8]。但是交变电磁场辅助激光焊接工艺存在作用深度只有 5 mm 及受磁滞影响严重的缺点，对熔池凝固结晶过程影响很小，且设备笨重，结构复杂[9-10]。

本文提出基于稳定磁场和定向电流产生的向上安培力辅助支撑熔池的方法，以改善熔池流动特性，达到抑制根部熔池滴落、提高焊接过程稳定性、提升焊缝成型质量和焊接效率的目的，最终将激光单道焊接双面成型良好的厚度提升至 30 mm。

2 试验设备及方法

2.1 试验材料

选用 16 mm 和 30 mm 厚的 316L 不锈钢，尺寸规格均为 300 mm×40 mm，表 1 为试件化学成分表。

表 1 316L 不锈钢的化学成分（质量分数）

Table 1 Chemical composition of 316L stainless steel (mass fraction) unit：%

316L	C	Si	Mn	S	P	Ni	Cu	N	Mo	Fe
Mass fraction	0.022	0.54	0.032	0.001	16.7	10.2	0.23	0.02	2.12	Bal.

收稿日期：2020-08-21；**修回日期**：2020-10-05；**录用日期**：2020-10-26

基金项目：国家重点研发计划（2018YFB1107905）

*E-mail：hdgychen@163.com

2.2 试验设备与方法

电磁辅助激光焊接厚板示意图如图 1 所示。从图 1 可知，本次试验设备可分为三部分，分别为电磁辅助焊接系统、激光焊接系统和熔池特征拍摄系统。在进行试验时，首先将试件夹紧在夹具上，并在试件两端与夹具接触处添加绝缘块以达到绝缘的目的。磁场能量是由吸附固定在虎钳两端的永磁铁产生的，两永磁铁竖直放置，N 极对 N 极，S 极对 S 极。试件放在永磁体上方约 4 mm，通过旋转虎钳螺丝，调整磁铁间距，可以改变磁场中试件的磁感应强度。当磁铁间距为 68 mm 时，使用型号为 SJ700 GAUSSMETER 的便携式数字高斯计测量试件中心处的磁场强度，测量值为 200 mT。根据安培定则，可知磁场的方向与试件电流方向应使得安培力竖直向上。大电流发生器通过铜导线与试件两端相连。

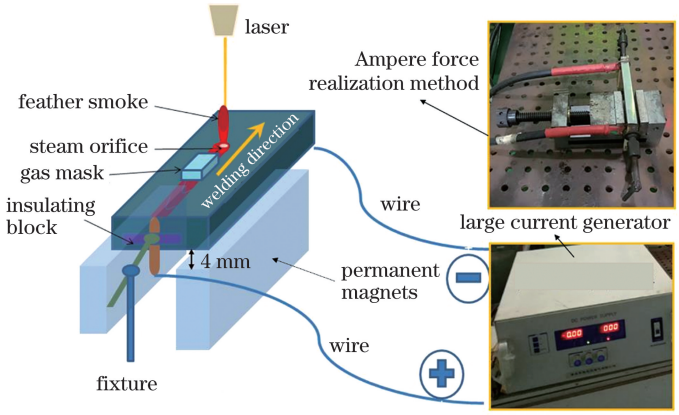

图 1 电磁辅助焊接装置示意图

Fig. 1 Schematic diagram of electromagnetic auxiliary welding device

电磁辅助焊接系统提前打开，电流从零升至指定电流大小需要 3～8 s，待电流稳定后启动激光焊接系统。激光焊接系统包括光纤激光器、焊接机器人及吹气装置等。本次试验的激光器采用 IPG 公司生产的 YLS-20000-CL 光纤激光器，最大输出功率为 20 kW，激光焊接头安装在 KUKA 公司生产的六自由度机器人手臂上，保护气体采用质量分数为 99.99%的氮气，保护气流量设为 25 L/min。

在焊接开始前，提前打开熔池特征拍摄系统，以实现对熔池焊接全过程的拍摄，该系统包括 808 nm 半导体激光器、滤光片、扩束镜和高速相机。半导体激光器的最大输出功率为 30 W，激光波长为 808 nm±3 nm，试验过程中采用了 808 nm±3 nm 窄带通滤光片。高速相机的型号为 Fastcam-SA4，拍摄帧数为 3600 frame·s^{-1}，分辨率为 1024 pixel×1024 pixel，高速相机拍摄方式如图 2 所示。

试验先用 16 mm 316L 不锈钢抑制根部滴落缺陷，而后用 30 mm 316L 不锈钢研究激光单道焊透工艺的极限厚度。因为安培力大小主要与电流大小和磁场强弱相关，所以在电流或磁场大小不变的情况下，可以用另一变量来指代安培力的大小，例如在磁场强度不变的情况下，可用电流大小来指代安培力大小，电流越大，安培力越大，或在电流大小不变

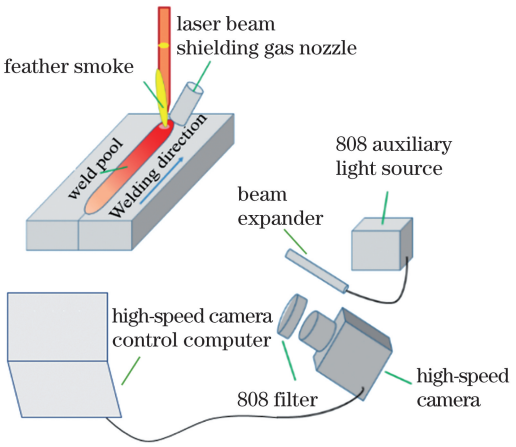

图 2 熔池特征拍摄系统示意图

Fig. 2 Schematic diagram of the molten pool feature shooting system

的情况下，可用磁铁间距来指代安培力大小，磁铁间距越小，安培力越大。

3 试验结果分析和讨论

3.1 安培力抑制根部熔池滴落缺陷研究

为了验证实验的准确性和可信性，避免电流或磁场对焊接过程的影响，同工艺参数条件下在 16 mm 厚不锈钢板上做了 4 组对比试验：激光焊接、激光＋电流焊接、激光＋磁场焊接、电磁辅助激

光焊接。焊接参数见表 2。

试验结果如图 3 所示。从采用激光焊接结果可以明显看出激光形成切割现象，焊缝无法成型。激光＋电流焊接与激光＋磁场焊接的结果很相似，都是焊缝虽然勉强成型，但都存在非常严重的滴落缺陷，焊接过程不稳定。国内外已经有很多学者对引入电流和磁场的激光焊接过程进行了研究，经查阅文献，可知电流或磁场对激光焊接的影响更多体现在改变焊接接头力学性能，改变焊缝组织形貌，对熔池的支撑作用较小[11-13]。只有采用激光＋电流＋磁场的方法，才能很好地抑制熔池的滴落，焊缝成 Y 型，取得良好的焊缝形貌和焊接质量。

表 2 验证电磁辅助激光厚板稳定焊接真实作用力为安培力的焊接实验参数

Table 2 Welding experimental parameters to verify that the real force of electromagnetic assisted laser welding for thick plate is Ampere force

Serial number	Power /kW	Focal length / mm	Welding speed / (m·min^{-1})	Magnet distance / mm	Current /A	Flow rate of N_2 / (L·min^{-1})
Laser welding	15.8	＋15	0.6	–	–	25
Laser＋Current	15.8	＋15	0.6	–	520	25
Laser＋Magnet	15.8	＋15	0.6	68	–	25
Laser＋Current＋Magnet	15.8	＋15	0.6	68	520	25

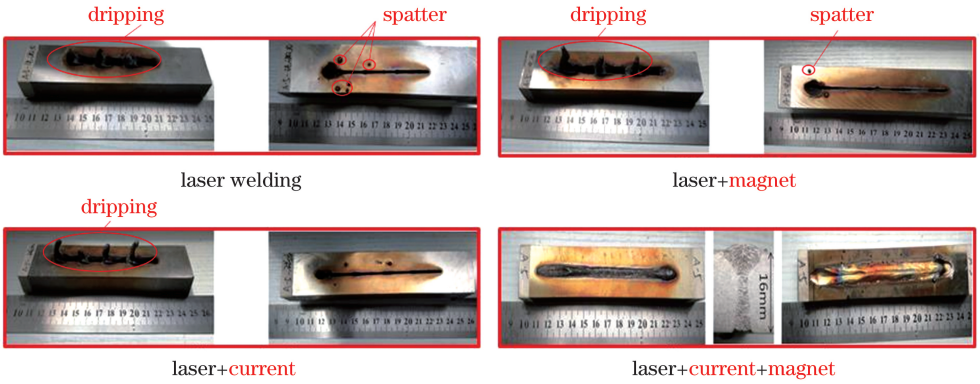

图 3 电磁辅助激光焊接工艺对比试验和焊缝形貌

Fig. 3 Comparison test of electromagnetic assisted laser welding process and weld morphology

电磁场的同时存在对抑制激光焊接厚板根部熔池滴落有积极作用，为了进一步研究安培力对焊接结果的影响，在只改变电流大小的情况下进行了工艺试验，试验参数如表 3 所示。焊接结果如图 4 所示。在 420 A 电流的情况下，根部熔池会产生部分均匀滴落，焊缝底部平齐无驼峰，上表面焊缝塌陷；在 445 A 电流的情况下，根部熔池滴落缺陷有所好转，但仍有少量滴落，上表面焊缝塌陷；在 470 A 电流的情况下，根部熔池滴落得到抑制，焊缝底部平齐但有少许凸起，焊缝形貌呈钉子头；在 495 A 电流的

表 3 磁场不变时电磁辅助激光厚板焊接 16 mm 316L 不锈钢试验参数

Table 3 Test parameters of 16-mm 316L stainless steel welded by electromagnetic assisted laser in constant magnetic field

Serial number	Power /kW	Focal length / mm	Welding speed / (m·min^{-1})	Magnet distance / mm	Current /A	Flow rate of N_2 / (L·min^{-1})
A-1	15.8	＋15	0.6	68	420	25
A-2	15.8	＋15	0.6	68	445	25
A-3	15.8	＋15	0.6	68	470	25
A-4	15.8	＋15	0.6	68	495	25
A-5	15.8	＋15	0.6	68	520	25

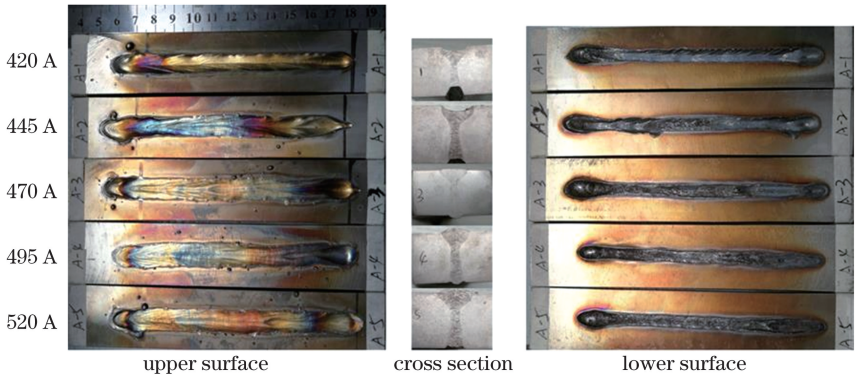

图 4　磁场不变时安培力对抑制根部熔池滴落缺陷的影响

Fig. 4　Effect of Ampere force in constant magnetic field on the suppression of dripping defects in the root molten pool

情况下，焊缝整体均匀，成型良好，焊缝形貌为 Y 字型，根部也无凸起现象；在 520 A 电流的情况下，熔池被安培力向上顶起，焊缝底部发生轻微向上凹陷现象。

通过上述的 4 组对比试验和电磁辅助激光焊接（只改变电流）试验，基本可以确定是安培力抑制了根部熔池滴落，改变了焊缝形貌。

为了证实试验的可信性，进一步针对电流大小不变，只改变磁场强度的情况进行了补充试验，焊接参数如表 4 所示，焊接结果如图 5 所示。在磁铁距离为 65 mm 的情况下，安培力过大，导致熔池被安培力向上顶起，根部发生向上凹陷的现象；增大磁铁距离，减小焊缝处的磁感应强度，在磁铁距离为 68 mm 的情况下，根部没有发生滴落缺陷，根部出现均匀的凸起现象，焊缝成型良好；进一步减小磁感应强度，在磁铁距离为 71 mm 的情况下，根部出现部分滴落，根部无明显凸起现象，上部焊缝产生了塌陷缺陷。

表 4　电流不变时电磁辅助激光焊接 16 mm 316L 不锈钢试验参数

Table 4　Test parameters of electromagnetic assisted laser welding of 16-mm 316L stainless steel at constant current

Serial number	Power /kW	Focal length / mm	Welding speed / (m·min^{-1})	Magnet distance / mm	Current /A	Flow rate of N_2 / (L·min^{-1})
B-1	15.8	+15	0.6	65	470	25
B-2	15.8	+15	0.6	68	470	25
B-3	15.8	+15	0.6	71	470	25

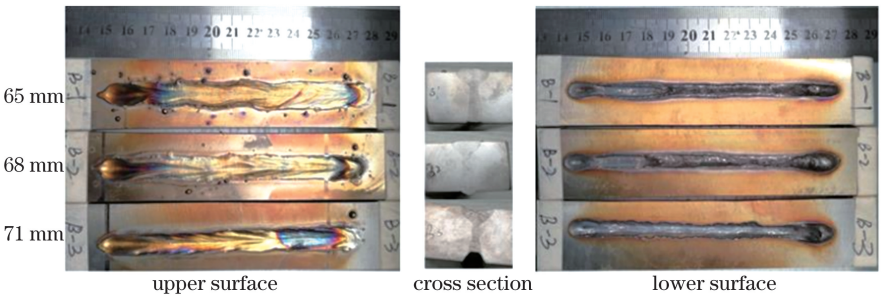

图 5　电流不变时安培力对抑制根部熔池滴落缺陷的影响

Fig. 5　Effect of Ampere force at constant current on the suppression of dripping defects in the root molten pool

根据上述电磁辅助激光焊接 16 mm 316L 不锈钢板试验，可知在试验中是安培力而不是电流或磁场抑制了根部熔池滴落，在安培力存在的情况下，即使发生滴落，根部熔池也是均匀滴落，焊缝根部基本平齐，故能保证焊缝的成型，不会出现切割现象。因此通过优化电磁工艺参数，可以很好地保证焊缝成型质量。

3.2　30 mm 不锈钢激光单道焊透试验

接着，进行 30 mm 不锈钢激光单道焊透工艺试验，旨在探究激光单道焊接厚板厚度极限，实现更大厚度的激光单道焊接双面成型。所有焊接参数除电流外均保持一致，依次逐步增大电流，焊接结果如

图 6 所示。焊接过程中电流稳定在 2000 A 时，焊缝根部完全熔透，焊缝根部出现周期性根部驼峰；当电流升高到 2300 A 时，焊缝成型质量最佳，呈现 Y 字形貌，焊缝根部无驼峰；当电流升高到 2600 A 时，焊缝深度基本达到 30 mm，根部焊缝为周期性焊透，焊缝宽度为 4 mm；当电流升高到 2900 A 时，焊缝深度为 26 mm，焊缝宽度为 3 mm，焊接过程未焊透；当电流升高到 3100 A 时，焊缝深度为 22 mm，焊缝宽度为 3.5 mm。

通过试验结果对比可知，当电流从 2600 A 升高到 2900 A 再升高到 3100 A 时，未焊透距离也从 0 升高到 4 mm 再升高到 8 mm，电流大小与未焊透距离成正相关，安培力越大，未焊透的距离也越大，安培力的大小影响着焊缝的成型，而安培力的大小对焊缝的宽度影响不大。如果电流过小，安培力则不足以支撑熔池，使得焊缝出现周期性驼峰，不利于焊接的稳定性；随着电流的增大，安培力增大，安培力如果过大，会导致熔池向上的支撑力过大，进而导致能量无法向下传递，导致材料不能完全焊透。只有选择适当的电流大小，产生大小合适的安培力，才能在抑制熔池滴落，形成良好的焊缝，同时确保材料完全焊透。综上可知，安培力可以有效抑制厚板焊接过程中的熔池滴落缺陷，保证了焊接稳定性和焊缝成型质量，通过设定合适的工艺参数，对于 30 mm 不锈钢板可以做到激光单道焊接一次成型，极大地提高了焊接效率。

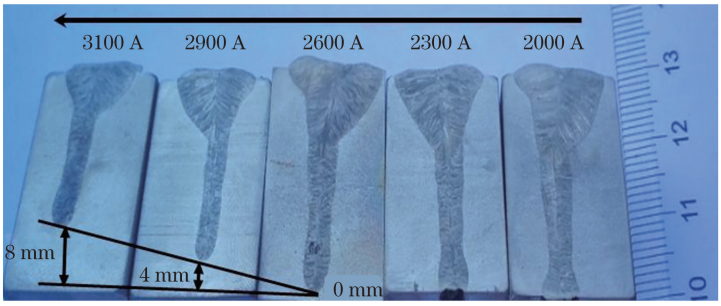

图 6　安培力对 30 mm 厚板焊接熔池深度和焊缝成型质量的影响

Fig. 6　Influence of Ampere force on the depth of the weld pool of 30-mm thick plates and the quality of weld formation

3.3　熔池流动行为分析

本次试验中运用高速相机对 16 mm 厚板焊接过程中根部熔池的流动行为进行了拍摄，拍摄结果如图 7 所示。图 7(a)、(b)、(c)中根部凸起比较小，体积也相对稳定，图 7(d)、(e)中根部凸起严重，但是没有发生熔池滴落的现象，图 7(f)中根部凸起已经变小，熔池稳定。在高功率激光焊接厚板无外力辅助的情况下，根部受力不平衡，根部会形成明显的凸起，在重力的作用下，熔池滴落。在有安培力辅助的情况下，安培力并不能抑制根部的凸起，安培力只是抑制了熔池的滴落，根部熔池凸起之后，在安培力和熔池表面张力的共同作用下，熔池向后回流到了

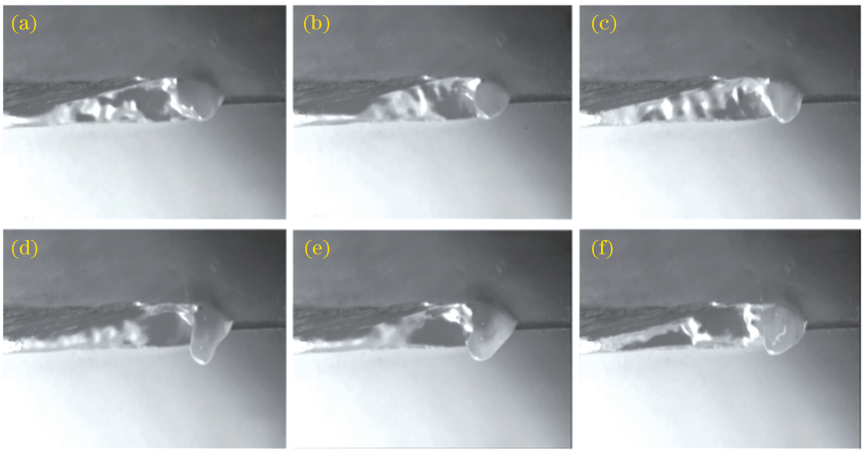

图 7　电磁辅助激光厚板焊接根部熔池流动行为。(a) t=0 ms；(b) t=300 ms；(c) t=600 ms；(d) t=900 ms；(e) t=1200 ms；(f) t=1500 ms

Fig. 7　Flow behavior of the molten pool at the root of electromagnetic-assisted laser thick plate welding. (a) t=0 ms; (b) t=300 ms; (c) t=600 ms; (d) t=900 ms; (e) t=1200 ms; (f) t=1500 ms

焊缝中，而无其他缺陷，最终获得了成型良好的焊缝。整个过程中，根部熔池的前端凸起最严重，因而需要最大的支撑力。

激光焊接开始时，试件逐渐熔化形成熔池，熔池逐渐增大，此时根部熔池表面向下凸起，凸起逐渐长大，这是因为凸起距离磁铁仍有一定距离，所以安培力较小，和熔池表面张力不足以平衡熔池向下的合力。随着焊接的进行，根部熔池凸起越来越大，根部熔池凸起位置越来越接近磁铁，不断增大的安培力和表面张力一起抑制了根部熔池凸起的趋势，根部熔池越来越大，直至达到并维持熔池动态稳定过程。此时熔池前端熔化速率等于后端凝固速率，熔池体积达到最大，根部熔池凸起依然存在，安培力的存在抑制了根部熔池凸起继续增大，避免了熔池凸起处滴落的缺陷，熔池在合力的作用下向后回流到焊缝中，最终保证了焊缝的成型。

4 结 论

利用电磁辅助激光焊接厚板方法，对 16 mm 和 30 mm 316L 不锈钢开展根部熔池滴落缺陷抑制工艺试验和熔池流动行为研究，得到了以下结论。

1）在 16 mm 不锈钢抑制根部熔池滴落缺陷试验中，单独外加电流或者磁场时都不能有效抑制激光单道焊接厚板时产生的根部熔池滴落缺陷，只有同时施加恒定电磁场，产生稳态的安培力，才能抑制熔池滴落。在焊接过程中安培力能够有效抑制熔池滴落，使得焊缝良好成型，确保了焊接质量，提高了焊接效率。

2）在 30 mm 不锈钢激光单道焊透工艺试验中，结果证实恒定电流加恒定磁场的电磁辅助激光焊接工艺方法是可行的，该方案可为超厚板激光焊接工艺开发提供参考。在焊接过程中，安培力不仅可以抑制熔池滴落，还可以明显改变熔深，电流为 2300 A 时，实现的激光单道焊接厚板，双面成型良好，焊缝成型质量最佳，呈现 Y 字形貌，焊缝根部无驼峰。

3）外加的安培力并不能阻止焊接过程中根部凸起的形成，只是与表面张力一起抑制了熔池向下滴落，并促使凸起熔池回流到焊缝区域，进而保证了有效的焊缝成型。

参 考 文 献

[1] Peng J, Xu H Q, Wang X X, et al. Numerical simulation of influence of welding speed on dynamic behavior of laser welding molten pool with filler metal [J]. Chinese Journal of Lasers, 2020, 47(3): 0302005.
彭进, 许红巧, 王星星, 等. 焊接速度对填材填充激光焊接熔池动态行为影响的数值模拟[J]. 中国激光, 2020, 47(3): 0302005.

[2] Huang Y, Huang J, Nie P L. Microstructures and textures of 6016 and 5182 aluminum laser welded joints[J]. Chinese Journal of Lasers, 2019, 46(4): 0402003.
黄毅, 黄坚, 聂璞林. 6016 和 5182 铝合金激光焊接接头的组织与织构[J]. 中国激光, 2019, 46(4): 0402003.

[3] Atabaki M M, Yazdian N, Ma J, et al. High power laser welding of thick steel plates in a horizontal butt joint configuration[J]. Optics & Laser Technology, 2016, 83: 1-12.

[4] IPG set to ship 100 kW laser [EB/OL]. (2012-11-01) [2020-08-01]. http://optics.org/news/3/10/44.

[5] Li S C. Study on the coupling behavior between metallic vapor and melt pool during deep penetration welding with 10-kW level laser [D]. Changsha: Hunan University, 2014.
李时春. 万瓦级激光深熔焊接中金属蒸气与熔池耦合行为研究[D]. 长沙: 湖南大学, 2014.

[6] Zhang M, Chen G, Zhou Y, et al. Direct observation of keyhole characteristics in deep penetration laser welding with a 10 kW fiber laser[J]. Optics Express, 2013, 21(17): 19997-20004.

[7] Zhang M J, Zhang Y Z, Mao C, et al. Experiments on formation mechanism of root humping in high-power laser autogenous welding of thick plates with stainless steels [J]. Optics & Laser Technology, 2019, 111: 11-19.

[8] Bachmann M, Avilov V, A. Gumenyuk, et al. Experimental and Numerical Investigation of an Electromagnetic Weld Pool Control for Laser Beam Welding. Physics Procedia, 2014, 515-524.

[9] Avilov V, Fritzsche A, Bachmann M, et al. Full penetration laser beam welding of thick duplex steel plates with electromagnetic weld pool support [J]. Journal of Laser Applications, 2016, 28(2): 022420.

[10] Bachmann M, Avilov V, Gumenyuk A, et al. Numerical assessment and experimental verification of the influence of the Hartmann effect in laser beam welding processes by steady magnetic fields [J]. International Journal of Thermal Sciences, 2016, 101: 24-34.

[11] Zhang X, Wu S, Xiao R, et al. Homogenisation of chemical composition and microstructure in laser filler wire welding of AA 6009 aluminium alloy by *in situ* electric current stirring [J]. Science and Technology of

Welding and Joining, 2016, 21(3): 157-163.

[12] Cao L C, Yang Y, Jiang P, et al. Optimization of processing parameters of AISI 316L laser welding influenced by external magnetic field combining RBFNN and GA[J]. Results in Physics, 2017, 7: 1329-1338.

[13] Sun Q J, Li J Z, Liu Y B, et al. Formation, microstructure, and properties of electromagnetic field-assisted SUS316L austenite stainless steel laser narrow-gap joint[J]. Chinese Journal of Lasers, 2020, 47(10): 1002005.
孙清洁, 李军兆, 刘一搏, 等. 电磁场辅助 SUS316L 不锈钢扫描激光窄间隙焊接接头成形及组织性能[J]. 中国激光, 2020, 47(10): 1002005.

Electromagnetic-Assisted Single-Pass Laser Welding of a 30-mm Thick Plate

Chen Genyu[1,2*], Wang Jingru[1], Qi Yi[3], Li Wei[1], Zhong Peixin[1], Dong Li[1]

[1] *Laser Research Institute, Hunan University, Changsha, Hunan* 410082, *China*;

[2] *State Key Laboratory of Advanced Design and Manufacturing for Vehicle Body, Hunan University, Changsha, Hunan* 410082, *China*;

[3] *School of Mechanical Engineering, Hubei University of Arts and Science, Xianyang, Hubei* 441100, *China*

Abstract

Objective Single-pass laser welding double-sided forming technology has the advantages of small welding deformation, high welding strength, large welding aspect ratio, and high welding efficiency. Under normal circumstances, the thickness limit of a sheet with double-sided welding in a single pass is 13 mm. When the sheet thickness reaches 15 mm or more, the biggest problem is to no longer optimize the process parameters to obtain a good weld seam; however, after the laser power exceeds the threshold and laser energy, steam, plasma, and other coupling behaviors in the keyhole are complex, the root molten pool drips and the weld is difficult to form. This paper proposes a method of using the upward Ampere force generated by a stable magnetic field and directional current to assist in improving the flow characteristics of the molten pool and suppressing the dripping of the root molten pool; improving stability of the welding process, quality of weld formation, and welding efficiency; and greatly improving the thickness limit of thick plates in single-pass laser welding.

Methods The experimental material used in this study is 316L stainless steel, and the specifications of the specimens are 300 mm × 40 mm × 16 mm and 300 mm × 40 mm × 30 mm. The magnetic field is generated by a permanent magnet attached to the vise, and direct current is generated by a large current generator. In this experiment, 16-mm 316L stainless steel was first used to study the root dripping defects, and then 30-mm 316L stainless steel was used to investigate the ultimate thickness of laser single-pass penetration. In the study of 16-mm 316L stainless steel to suppress root dripping defects, four sets of comparative tests were first carried out: laser welding, laser current welding, laser magnetic field welding, and electromagnetic assisted laser welding. In order to ensure accuracy and credibility of the test and avoid the influence of current or magnetic field on the welding process, the single-factor experiment method is used to change only the magnetic field or current and keep other process parameters unchanged. The question is whether the Ampere force is the real force when electromagnetic-assisted laser welding of thick plates is studied, and the flow behavior of the molten pool at the root is photographed by a high-speed camera. In the study of the thickness limit of the 30-mm 316L stainless steel single-pass laser penetration process, the Ampere force was changed by variable current and constant other process parameters. The influence of the Ampere force on the depth of the 30-mm thick plate welding pool and weld formation quality impact was studied.

Results and Discussions Among the results of the four sets of comparative tests (Fig. 3), only the test method of electromagnetic-assisted laser welding can achieve significantly better welding results than other sets of results. The weld seam is Y-shaped; weld formation and weld quality is good. Through the test results of electromagnetic-assisted laser welding of 16-mm 316L stainless steel plates (Fig. 4 and Fig. 5) and by adjusting the magnitude of the magnetic field or current, the weld morphology can be significantly changed. Therefore, in the experiments, it is the Ampere force rather than the current or magnetic field that inhibits the root molten pool dripping. With the presence of Ampere force, even if the dripping defect occurs, the root molten pool drips evenly and the root of the

weld seam is flush, which can ensure formation of the weld without cutting. The high-speed camera shooting result (Fig. 7) shows the flow behavior of the root molten pool during electromagnetic-assisted thick plate laser welding, indicating that the Ampere force cannot suppress root protrusion. However, the Ampere force suppresses dripping of the molten pool and the root molten pool protrusions after that. Under the combined action of the Ampere force and the surface tension of the molten pool, the molten pool flows back into the weld without other defects and a well-formed weld is obtained finally. Through the experiment results of electromagnetic-assisted laser welding of 30-mm 316L stainless steel plates (Fig. 6), it can be seen that the Ampere force affects the depth of the weld, but hardly affects the width of the weld. Only by selecting the appropriate Ampere force, the dropping in the molten pool can be suppressed thereby forming a good weld and ensuring that the material can be completely welded. By setting the appropriate process parameters, a single-pass laser welding can be achieved for a 30-mm stainless steel plate, which greatly improves the welding efficiency.

Conclusions In this paper, electromagnetic-assisted laser welding of thick plates is used to carry out root molten pool dripping defect suppression process experiments and molten pool flow behavior research on 16-mm and 30-mm 316L stainless steel. In the experiments of 16-mm stainless steel to suppress the dripping defect of the root molten pool, neither the applied current nor the magnetic field alone can effectively suppress the root molten pool dripping defects generated during the single-pass laser welding of thick plates. Only by applying a constant electromagnetic field at the same time, the steady-state Ampere force generated can inhibit the dripping of the molten pool. During the welding process, the Ampere force can effectively inhibit the dripping of the molten pool, ensure good formation of the weld seam, ensure good welding quality, and improve the welding efficiency. In the 30-mm stainless steel laser single-pass penetration process test, the electromagnetic-assisted laser welding process method at constant current and constant magnetic field is feasible, laying the foundation for the development of ultra-thick plate laser welding process. During the welding process, the Ampere force can not only inhibit the dripping of the molten pool, but also significantly change the depth of the molten pool. The attached Ampere force cannot prevent the formation of root protrusions during the welding process; however, together with surface tension, it inhibits the downward dripping of the molten pool and helps the protrusion molten pool reflow to the weld area, ensuring effective weld formation.

Key words laser processing; laser welding; electromagnetic field; thick plate; molten pool dripping

OCIS codes 140.3390; 140.3510; 350.3390